

Production of Heavy Nuclei in the Par and Barbel Devices*

GEORGE I. BELL

University of California, Los Alamos Scientific Laboratory, Los Alamos, New Mexico

(Received 19 April 1965)

In the Par and Barbel thermonuclear devices, heavy nuclei up to $A=257$ were produced by the exposure of U^{238} to intense neutron fluxes. If one tries to interpret the resulting abundance as a function of mass number by assuming that all higher nuclei resulted from multiple neutron capture in U^{238} , there are difficulties in reconciling the high- A data with standard semiempirical mass formulas and neutron-capture cross-section theories. Neither the general trend of abundance as a function of A , nor the odd-even fluctuation (for $A > 249$) which is superimposed on this trend, is consistent with standard theory. In this paper we explore the suggestion that the high-mass isotopes resulted from neutron capture in odd- Z nuclei (Pa and Np). We adopt a simplified model of the thermonuclear devices in which deuterium plus tritium burns to completion and resulting neutrons are captured by various heavy nuclei. We first estimate, in Sec. II, the number of uranium nuclei which will be transformed to odd Z by the reactions $U^{238}(n,p)Pa^{238}$; $U^{238}(d,n)Np^{239}$, and $U^{238}(d,2n)Np^{238}$. A production of about 10^{-3} Pa/U and $\leq 10^{-3}$ Np/U is found and it is estimated that roughly these ratios will be available as targets for multiple neutron capture. In Sec. III statistical theory is used together with Seeger's semiempirical mass formula to calculate 20-keV neutron-capture cross sections for the nuclei $91 \leq Z \leq 93$, $238 \leq A \leq 257$. The average odd- Z cross sections are systematically larger than the even Z , and those of Np are larger than Pa. The mass-yield curve can then be calculated for various neutron-flux values and in Sec. IV the results are compared with experiment. For both Par and Barbel, good agreement with the experimental abundance data is found using a 20-keV exposure of 7×10^{24} neutrons/cm². For Par, a Np/U ratio of 10^{-3} is required while for Barbel the corresponding ratio is about 5×10^{-4} . In both cases the light end of the mass curve ($A < 248$) is due to the uranium capture chain, while the heavy end ($A \geq 250$) arises from capture by Np. A comparison is also made with less complete data from the Mike device, and it is found that for $A \geq 245$ the data can be fit for $\varphi = 6 \times 10^{24}$ neutrons/cm² with $Np/U \approx 1.5 \times 10^{-4}$. We conclude that the formation of odd- Z nuclei which undergo multiple neutron capture permits one to understand the mass-yield curves using standard semiempirical mass formulas and conventional capture-cross-section theory.

I. INTRODUCTION AND SUMMARY

IN the intense neutron fluxes which are found in thermonuclear explosions, heavy nuclei may be synthesized by multiple neutron capture. The first thermonuclear explosion (Mike) produced nuclei with masses up to $A=255$, which were detected in the debris by radiochemical techniques.¹ More recently, as part of the Atomic Energy Commission's Plowshare Program, some low-yield devices have been exploded underground for the purpose of producing heavy nuclei. In two recent experiments of this kind (Par,² and Barbel³), nuclei through mass 257 were found by radiochemical analysis of excavated debris. Some of the more abundant nuclei were identified on mass spectrographs.

The primary purpose of these latter experiments has been the production of new and interesting heavy nuclei. However, from an analysis of the abundances of the heavy nuclei which are produced it should also be possible to draw some conclusions regarding the neutron capture and fission cross sections of the nuclei which are involved. A straightforward analysis leads to immediate problems. In particular one concludes that the neutron-capture cross sections are not noticeably

decreasing as one adds neutrons, a conclusion which is at variance with standard notions of the behavior of neutron binding energies and capture cross sections, and which will be discussed at length in the body of this paper. The essential features of this straightforward analysis can be appreciated as follows. In all of the devices which we are considering (Mike, Par, and Barbel), the primary target material for neutron capture is U^{238} , and it is natural to expect that the successive neutron captures lead to U^{239} , U^{240} , etc. Thus let us consider the multiple capture of neutrons, starting from U^{238} . Let $n(E,t)$ be the neutron density as a function of energy and time, $\sigma_{n,\gamma^i}(E)$ the neutron capture cross section for a uranium nucleus of mass number $238+i$ and a neutron of energy E , and N_i the final abundance of the mass $238+i$ nucleus. If we assume that the neutron density is independent of position (so that each nucleus sees the same density of neutrons) and that σ_{n,γ^i} is independent of i , then letting

$$\int dt \int dE \sigma_{n,\gamma}(E) v n(E,t) = x$$

it is easy to show that

$$N_i = N_0 (x^i / i!) e^{-x}. \quad (1)$$

The disturbing feature is that such a simple expression gives (except for odd-even effects) values of N_i which are in rather good agreement with the experimental

* Work performed under the auspices of the U. S. Atomic Energy Commission.

¹ H. Diamond *et al.*, Phys. Rev. **119**, 2000 (1960).

² D. W. Dorn and R. W. Hoff, Phys. Rev. Letters **14**, 440 (1965).

³ Los Alamos Radiochemistry Group, Phys. Rev. Letters **14**, 962 (1965).

N_i as seen on Mike, Par, and Barbel. In this fitting, N_0 and x are treated as adjustable parameters. This agreement tempts one to conclude that the capture cross sections are roughly constant as a function of i . Such a conclusion was first published by Cameron⁴ based on the Mike N_i values.¹

The Mike device was large and complicated and the assumption of constant neutron density throughout the uranium should be questioned. If one allows the density to vary with position then one can fit the observations with capture cross sections which decrease with i . The highest i nuclei will then be made in small regions of peak density. For example, with two neutron-density regions the Mike data can be fit with capture cross sections which decrease a factor of two between U^{238} and U^{235} .⁵ Thus from the Mike data because of unknown variations of neutron density with position it is hard to draw conclusions regarding the capture cross sections.

In both the Par and Barbel devices, on the other hand, small targets of U^{238} were deliberately used and the neutron flux in the uranium should be nearly constant. Since the constant cross-section approximation, Eq. (1), gives reasonable agreement (except for odd-even effects) with Par and Barbel data, it is apparent that the problem which we have disposed of for Mike by invoking a spatially varying density, has returned with renewed vigor.

The odd-even effects furnish a clue as to an escape from this constant-cross-section conclusion. If we neglect the possibility of fission, then the capture cross section for an odd- A uranium nucleus is expected to be higher than that for an adjacent even- A uranium nucleus. This will be discussed in detail later. The neglect of fission is believed to be justified for neutron energies less than 100 keV, where most of the captures probably take place. Now a nucleus with high-capture cross section will appear with a relatively low abundance in the final debris and we thus expect odd- A nuclei to be relatively less abundant than even- A nuclei. By this we mean that if a smooth curve is drawn through the N_i values for i even, the points for i odd will lie below this curve. Such an odd-even effect is indeed found for Mike, Par, and Barbel for $i \lesssim 11$ ($A = 249$) but for greater i , the alternation appears to have reversed, and the odd- A nuclei are relatively more abundant. Diamond and Fields⁶ appear to have been the first to suggest that this reversal could be understood if the nuclei with large i had been produced by neutron capture in an odd- Z mass chain; for example, if some of the uranium nuclei were to capture protons, thus becoming neptunium, and neutron captures were to then carry one to successively higher neptunium isotopes. Since the mass analysis of

debris is made after the uranium or neptunium nuclei have β decayed to higher Z nuclei, it furnishes no evidence on whether odd- or even- Z nuclei are capturing the neutrons. Capture in an odd- Z mass chain would be expected to lead to a reversal of the odd-even effect, i.e., to relatively high odd- A abundances.

The purpose of the present paper is to explore the competition between neutron capture in even- and odd- Z mass chains and to see if the Par and Barbel results can be understood on this basis. In Sec. II we first estimate how many odd- Z nuclei may be formed while thermonuclear reactions are taking place. We find that (n,p) reactions will produce about 10^{-3} protoactinium nuclei per uranium nucleus, while (d,n) , $(d,2n)$, and similar reactions will produce less than or about 10^{-3} neptunium nuclei per uranium nucleus.

In Sec. III we calculate the capture cross sections of the relevant nuclei ($91 \leq Z \leq 93$; $238 \leq A \leq 257$). Conventional statistical theory is used.^{7,8} The most important parameter is the density of levels of the compound nucleus. We use a Fermi gas level-density formula, with spin and pairing effects, as given by Newton⁹ and with two constants determined by fitting heavy nuclear level densities. Extrapolated neutron binding energies were taken from the tabulation of Seeger's semiempirical mass data.¹⁰ The neutron capture cross sections which are obtained (see Table II) show odd-even variations and decrease with increasing i . Averaging over odd-even pairs, the Np cross sections are largest, followed by Pa and U in that order.

In Sec. IV we use the calculated cross sections plus the estimates of Pa and Np production to see if the Par and Barbel data can be fit. Using 10^{-3} Np/U we obtain good agreement with the Par data while a ratio of 5×10^{-4} Np/U fits the Barbel data. The less complete Mike data can be fit with $Np/U \approx 1.5 \times 10^{-4}$.

II. PRODUCTION OF PROTOACTINIUM AND NEPTUNIUM

We assume that the region where synthesis of heavy nuclei takes place may be described as being initially a volume of deuterium and tritium which contains a small amount of uranium-238. By "small amount" we imply that the effect of the uranium on the neutronics in the volume is negligible. When they reach a sufficiently high temperature, the deuterons and tritons will react



to produce neutrons of about 14 MeV and α particles of about 3.5 MeV. The neutrons are then moderated by collisions with the various nuclei and they are

⁴ A. G. W. Cameron, Can. J. Phys. **37**, 322 (1959).

⁵ D. W. Dorn, Phys. Rev. **126**, 693 (1962).

⁶ P. R. Fields (private communication).

⁷ B. Margolis, Phys. Rev. **88**, 327 (1952).

⁸ A. M. Lane and J. E. Lynn, Proc. Phys. Soc. (London) **A70**, 557 (1957).

⁹ T. D. Newton, Can. J. Phys. **34**, 804 (1956).

¹⁰ P. Seeger, Nucl. Phys. **25**, 1 (1961).

available for neutron capture by uranium (or other) nuclei.

As a first approximation we assume that all the neutron capture reactions take place after the thermonuclear reactions are completed and after the neutrons have been moderated to energies $\lesssim 100$ keV. However during the time when the thermonuclear reactions are taking place, the uranium will be exposed to an intense fast neutron flux which will produce fission, $(n,2n)$, $(n,3n)$, and (n,p) reactions. In addition, collisions of the fast neutrons with d or t will lead to the possibility of energetic deuterons or tritons which can produce (d,γ) , (d,n) , $(d,2n)$, $(d,3n)$, (t,γ) , (t,n) , $(t,2n)$, and $(t,3n)$ reactions on uranium.

Let us first estimate the number of (n,p) reactions, which will lead to Pa. Suppose the initial deuteron and triton nuclear densities are $n_d(0)$ and $n_t(0)$, respectively, and that $n_d(0) = n_t(0)$. If for convenience we assume that the reaction proceeds to completion, then about $n_d(0)$ 14-MeV neutrons will be produced per unit volume. Initially, each neutron will have a mean free path, $\lambda_0 = [n_d(0)\sigma_d + n_t(0)\sigma_t]^{-1}$, where σ_d and σ_t are the deuteron and triton cross sections for 14-MeV neutrons, namely 0.8 b and 1.0 b, respectively. Even after the $d+t$ have been largely transmuted to He^4+n , the mean free path will be similar to λ_0 since the (n,He^4) and (n,n) cross sections are much the same. Thus each 14-MeV neutron may be given a lifetime $\tau = \lambda_0/v$. Denoting the density of 14-MeV neutrons by $n(14,t)$, we see that its time integral will be about $n_d(0)\lambda_0/v$ while the time integrated flux

$$\int_0^\infty n(14,t) v dt \simeq n_d(0) \lambda_0 \simeq 0.6 \times 10^{24} \text{ cm}^{-2}.$$

Note that this flux is independent of the initial deuteron density.

The cross section for $\text{U}^{238}(n,p)\text{Pa}^{238}$ has not been measured. However (n,p) cross sections have been reported¹¹ for 14-MeV neutrons on U^{235} (1.8 mb), Np^{237} (1.3 mb), and Pu^{239} (3.0 mb). For our reaction, somewhat less energy is available for the proton and we estimate $\sigma(n,p) \lesssim 1$ mb. The (n,p) cross section will decrease rapidly with decreasing neutron energy so that the flux of uncollided 14-MeV neutrons will be the major source of (n,p) reactions and we will neglect the collided neutrons.

Suppose now that the uranium is exposed to a flux $vn(E,t)$ of fast neutrons, including 14-MeV neutrons and those which have suffered one or more moderating collisions. Let $\sigma(E)$ and $\sigma'(E)$ be the cross sections for destruction of the U and Pa nuclei, respectively, and $\sigma_c(E)$ be the cross section for creation [by (n,p) reactions] of Pa. [If we consider only U^{238} and Pa^{238} , then $\sigma \simeq \sigma(n,f) + \sigma(n,2n) + \sigma(n,3n) + \sigma(n,p)$ and $\sigma_c = \sigma(n,p)$.

If U^{237} and U^{236} are explicitly considered together with (n,p) reactions thereon, the situation is more complicated but the essential conclusions are not altered.] Then letting $N_0(t)$ be the density of U^{238} and $N_0'(t)$ be the density of Pa^{238} , we have

$$\frac{dN_0(t)}{dt} = -N_0(t) \int dE \sigma(E) vn(E,t), \quad (2a)$$

$$\begin{aligned} \frac{dN_0'(t)}{dt} = & -N_0'(t) \int dE \sigma'(E) vn(E,t) \\ & + N_0(t) \int dE \sigma_c(E) vn(E,t). \end{aligned} \quad (2b)$$

If we denote

$$X(t) = \int dE \sigma(E) vn(E,t)$$

and similarly for X' and X_c , then starting from the initial conditions $N_0(0) = N$ and $N_0'(0) = 0$, the solutions of (2) yield

$$\frac{N_0'(t)}{N_0(t)} = \int_0^t X_c(t') \left[\exp \int_{t'}^t \{X(t'') - X'(t'')\} dt'' \right] dt'. \quad (3)$$

For $X' \simeq X$ we have

$$N_0'(t)/N_0(t) \simeq \int_0^t X_c(t') dt'. \quad (4)$$

Since Pa^{238} is not expected to be fissionable by thermal neutrons, σ is probably not far from σ' and therefore Eq. (4) is a reasonable estimate. For the (n,p) reaction we have $\int_0^\infty X_c(t') dt' \simeq 10^{-27} \int_0^\infty n(14,t) v dt \simeq 0.6 \times 10^{-3}$. In view of the uncertainties in the cross sections for $\text{U}^{238}(n,p)$ and Pa^{238} destruction, this may be taken to be about 10^{-3} . We thus conclude that exposure of the uranium to the fast-neutron flux leads to about 10^{-3} Pa per U nucleus remaining. Hence there will be about 10^{-3} as many Pa nuclei as U nuclei available to capture neutrons. It may be mentioned that multigroup calculations of the uranium destruction by the fast flux predict that of the order of 10% of the original U^{238} nuclei survive and are thus available to capture the moderated neutrons.

Let us next estimate the Np production. We first note that the time available for all reactions is short enough that β decay during the explosion will be a very small source of Np. The principal source of Np, we believe, arises from the fast deuterons resulting from collisions with the 14-MeV neutrons. In a collision with a 14.1-MeV neutron, a deuteron can acquire up to 12.5 MeV (a triton can acquire up to 10.6 MeV, and a proton up to 14.1 MeV). Only the fastest deuterons can penetrate the Coulomb barrier to react with uranium nuclei and we must now estimate the time integrated flux of fast deuterons.

When the thermonuclear burning begins we have

¹¹ R. F. Coleman *et al.*, Proc. Phys. Soc. (London) A73, 215 (1959).

equal numbers of tritons and deuterons present and the probability of a 14-MeV neutron colliding with a deuteron is about $\frac{1}{2}$. When the burning ends we have few deuterons present so the probability of collision with a deuteron is very small. The average probability of collision with a deuteron is thus about 0.25. Thus the source of deuterons receiving energy from 14-MeV neutrons is one quarter of the source of 14-MeV neutrons or $0.25n_d(0)$ per unit volume. From the differential scattering cross section,^{12a} the energy spectrum of this source of fast deuterons can be calculated. Let us call it $0.25n_d(0)S_d(E)$ with $S_d(E)$ the normalized source.

If a volume of deuterium and tritium is brought to its ignition temperature,^{12b} it will then rapidly heat itself to very high temperatures by means of the thermonuclear reactions. At sufficiently high temperatures, the main mechanism for energy loss by fast deuterons arises from nuclear interactions with other nuclei.¹³ To obtain an upper limit to the Np production we may take this to be the *only* mechanism of deuteron moderation. If we take a cross section for nuclear interaction between deuterons and other nuclei of 1 barn, and assume that one nuclear collision removes the deuteron from the energy range of interest, then the time integrated fast deuteron flux is

$$v \int n_d(E,t) dt = 0.125 S_d(E) \times 10^{24} \frac{\text{deuterons}}{\text{MeV cm}^2}. \quad (5)$$

From the differential cross section we have computed $S_d(E)$ and from this the fast deuteron flux shown in Fig. 1.

The actual deuteron flux will tend to be shifted to lower energies and to be smaller than shown in Fig. 1 because we have ignored the moderating effect of Coulomb collisions between the fast deuterons and other nuclei or electrons. On the other hand, it will be shifted to higher energies because the neutrons do not really all have 14.1 MeV, but rather a spread of energies depending on the center of mass motion of the reacting particles. On balance, we will regard the numbers of reactions computed using the fluxes in Fig. 1 as rough upper limits. In any actual device the reactions may be substantially less due to details of temperature, geometry, or other factors.

A similar flux could be obtained for fast tritons. Here, however, the spectrum would begin at 10.6 MeV instead of 12.5 and would be less effective in penetrating the barrier. Some fast protons will also be formed, starting from the $n(d,2n)p$ products or from

¹² (a) M. D. Goldberg, V. M. May and J. R. Stehn, *Brookhaven Report, BNL-400* (Office of Technical Services, Department of Commerce, Washington, D. C., 1963), 2nd ed., Vol. 1. (b) S. Glasstone and R. H. Lovberg, *Controlled Thermonuclear Reactions* (D. Van Nostrand Company, Inc., Princeton, New Jersey, 1960).

¹³ C. Longmire, *Elementary Plasma Physics* (John Wiley & Sons, Inc., New York, 1964).

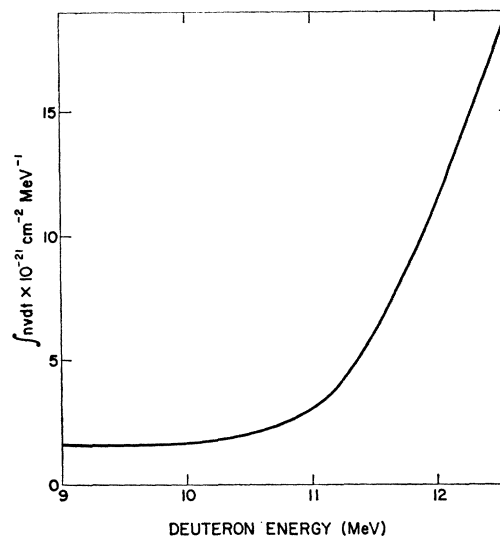


FIG. 1. Fast-deuteron flux in deuterons/cm² MeV ($\times 10^{21}$) resulting from burning of D+T.

protons originally present in the fuel. These also we will ignore.

Measurements of (d,γ) and $(d,2n)$ reactions on U^{238} have been reported by several authors.^{14,15} For the $(d,2n)$ reaction, we use the results of Wing *et al.*,¹⁵ as shown in Fig. 2. No good measurements of the $U^{238}(d,n)$ cross section have been reported, though some rough limits have been measured,¹⁴ and (d,n) cross sections of other heavy nuclei are known.¹⁶⁻¹⁸ To obtain further information on the (d,n) cross section, Dr. William Gibbs of this Laboratory performed some distorted-wave Born approximation calculations which give a ratio of $\sigma(d,n)$ to $\sigma(d,p)$. For incident deuteron energies of 12 and 14 MeV, the ratios $\sigma(d,n)/\sigma(d,p)$ were 0.2 and 0.5. Both were computed for $Q=2$ MeV, which means that the outgoing neutron or proton energy was taken to be equal to the incident deuteron energy plus 2 MeV. For purposes of the present estimate we have taken $\sigma(d,n)=0.2\sigma(d,p)$ together with values of $\sigma(d,p)$ from Ref. 15. The results are shown on Fig. 2. It will be observed that these cross sections have about the same energy dependence, given primarily by barrier penetration. For an estimate of the (d,γ) cross section we use 2% of the $(d,2n)$, which gives a value in reasonable agreement with experimental results (≈ 1.5 mb) at 14 MeV and a reasonable energy dependence.

If we multiplied one of the cross sections of Fig. 2

¹⁴ R. M. Lessler, University of California Radiation Laboratory Report No. UCRL-8439, 1958 (unpublished).

¹⁵ J. Wing, W. J. Ramler, A. L. Harkness, and J. R. Huizenga, *Phys. Rev.* **114**, 163 (1959).

¹⁶ W. M. Gibson, University of California Radiation Laboratory Report No. UCRL-3493, 1956 (unpublished).

¹⁷ E. V. Luoma, University of California Radiation Laboratory Report No. UCRL-3495, 1956 (unpublished).

¹⁸ L. M. Slater, University of California Radiation Laboratory Report No. UCRL-2441, 1956 (unpublished).

by the fast deuteron flux of Fig. 1 and integrated over energy, the result, which we denote by R , would give the probability that uranium-238 nuclei which were not undergoing other reactions would end up as Np^{238} or Np^{239} nuclei. If the destruction cross sections for the Np nuclei and for U^{238} were comparable then the ratio R would also about equal the number of Np nuclei surviving exposure to the fast neutron flux, divided by the number of surviving U^{238} nuclei. In fact, Np^{239} is probably not much more fissionable than U^{238} so that R for $\sigma(d,n)$ furnishes a good estimate of the surviving Np^{239} . Np^{238} , on the other hand, is highly fissionable so that the estimate R will be an upper limit to the Np^{238} remaining.

For the (d,n) reaction we find $\int \sigma[\int n v d t] d E_d \simeq 3 \times 10^{-4}$ while for the $(d,2n)$ process the corresponding integral is about 8×10^{-4} . In view of the uncertainties involved, we conclude that the surviving Np nuclei $\lesssim 10^{-3}$ times the surviving U nuclei, and that roughly comparable contributions will survive from the (d,n) and $(d,2n)$ reactions. The (d,γ) reaction would appear to give a negligible contribution $\sim 10^{-5}$ Np/U . Reactions with fast tritons should be considerably less effective than the deuteron reactions, because the tritons are less energetic.

III. CALCULATION OF NEUTRON-CAPTURE CROSS SECTIONS

A. General

Statistical theories of neutron capture have been given by Margolis,⁷ Lane and Lynn,⁸ Cameron,¹⁹ and others. We will use essentially the theory of Margolis, together with the correction, $S_1(\alpha)$, of Lane and Lynn which takes the fluctuations of neutron width into account. No spin-orbit interaction is taken into account and in general we will try to avoid refinements that do not seem significant for the present study.

Since we are most interested in the capture of neutrons having energies less than 100 keV we consider only s and p partial waves and ignore the possibility of inelastic scattering. In this energy region, $\sigma_{n,\gamma}$ varies roughly as $E^{-1/2}$ so that the product σv is a slowly varying function of neutron energy. Since only the product σv enters our calculations we may choose all the neutrons to have some single energy. In the numerical results to be reported we will take an arbitrary neutron energy of 20 keV because for this energy the contributions to $\sigma_{n,\gamma}$ of the s and p waves are comparable. We have, however, verified that our qualitative conclusions are quite insensitive to the choice of neutron energy. We also ignore the possibility that a nucleus under consideration may fission after absorbing a neutron. This should be a good approximation for all nuclei considered, except for the first few even- A

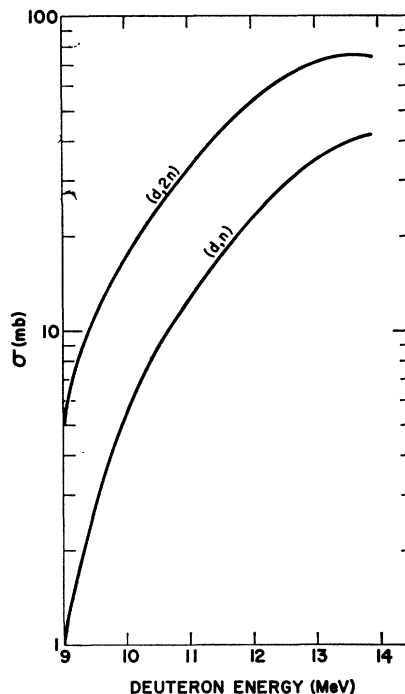


FIG. 2. Cross sections for deuterons reacting with uranium $\sigma(d,n)$ and $\sigma(d,2n)$.

neptunium nuclei, in particular Np^{238} and Np^{240} . For these nuclei, the capture to fission ratio will determine what fraction of the starting nuclei can proceed to further multiple capture, but in view of the uncertain state of theories of fission width we have not attempted to calculate the capture to fission ratios.

For capture by an even-even nucleus, we assume that the target has spin zero, while for capture from an even-odd, or odd-even nucleus we take the target spin to be $\frac{5}{2}$ as a reasonable average for the nuclei under consideration. For odd-odd nuclei we took an average spin of 3.

Let $T_l(E)$ be the penetration factor for neutrons of angular momentum l ; D_J the average level separation for compound nuclear levels of spin J ; Γ_γ^J the radiative capture width for levels of spin J ; and let $\xi_J = D_J(2\pi\Gamma_\gamma^J)^{-1}$. We compute a capture section averaged over many resonances, assuming a constant Γ_γ for these resonances, and a Porter-Thomas (χ^2 with one degree of freedom) distribution of neutron widths. The average neutron width per channel, $\bar{\Gamma}_n^{lJ}$ is $(D_J/2\pi)T_l$ and we call $\alpha_{l,J} = \Gamma_\gamma/\bar{\Gamma}_n^{lJ}$. The function $S_1(\alpha)$ is plotted in Ref. 8. Then for capture from a spin-zero nucleus we take

$$\sigma_{n,\gamma}(E) = \frac{\pi\lambda^2}{2} \left[T_0(E) \frac{2S_1(\alpha_{0,1/2})}{1 + \xi_{1/2}T_0(E)} + T_1(E) \left\{ \frac{2S_1(\alpha_{1,1/2})}{1 + \xi_{1/2}T_1(E)} + \frac{4S_1(\alpha_{1,3/2})}{1 + \xi_{3/2}T_1(E)} \right\} \right] \quad (6a)$$

¹⁹ A. G. W. Cameron in *Fast Neutron Physics*, edited by J. B. Marion and J. L. Fowler (Interscience Publishers, Inc., New York, 1963), Sec. V. M.

while for capture from a spin $\frac{5}{2}$ nucleus

$$\sigma_{n,\gamma}(E) = \frac{\pi\lambda^2}{12} \left[T_0(E) \left\{ \frac{5S_1(\alpha_{0,2})}{1+\xi_2 T_0(E)} + \frac{7S_1(\alpha_{0,3})}{1+\xi_3 T_0(E)} \right\} + T_1(E) \left\{ \frac{3S_1(\alpha_{1,1})}{1+\xi_1 T_1(E)} + \frac{10S_1(2\alpha_{1,2})}{1+2\xi_2 T_1(E)} + \frac{14S_1(2\alpha_{1,3})}{1+2\xi_3 T_1(E)} + \frac{9S_1(\alpha_{1,4})}{1+\xi_4 T_1(E)} \right\} \right]. \quad (6b)$$

We have assumed $T_i=0$, $i \geq 2$. For a spin 3 target, the numerical results turn out to be nearly identical to those for spin $\frac{5}{2}$ and therefore we will not consider the spin 3 case separately.

B. Penetration Coefficients

In Eqs. (6a) and (6b) T_0 and T_1 are functions of E . We ignore their possible variation with A since over the range of A which we consider, the variation is probably small and surely uncertain. For the results reported here we have used values of T_i suggested by optical model calculations of Beyster *et al.*,²⁰ namely $T_0=0.07$ and $T_1=0.01$ for $E_n \simeq 20$ keV. These values give a cross section for compound-nucleus formation, $\sigma_c = 3.2$ b and if we assume $T_i \propto E^{l+1/2}$, then $\sigma_c = 5.0$ at 5 keV and 10.4 at 1 keV. These values seem too small by $\sim 30\%$, when compared with $(1+\alpha)\sigma_f$ as determined for U²³³, U²³⁵, and Pu²³⁹.²¹ The average of Γ_n^{0J}/D_J at 1 eV for the heavy nuclei ($A \geq 232$) is about 1.1×10^{-4} ,^{21,22} which would give $T_0 \simeq 0.10$ at 20 keV.

More detailed optical-model calculations of penetration factors have been reported by Auerbach and Perey²³ for energies ≥ 100 keV. Although their calculations include surface absorption and spin-orbit coupling they are for spherical nuclei and hence still may not be accurate for the deformed heavy nuclei. Extrapolating their values to lower energies as $E^{l+1/2}$ we find at 20 keV $T_0=0.05$ or 0.08 for the Bjorklund, Fernbach, and Perey, Buck parameters, respectively, and $T_1 \simeq 0.027$.

Using the largest T_i values mentioned above, namely, for 20 keV, $T_0=0.10$, $T_1=0.027$, we find $\sigma_c = 5.9$, 7.8, 15.1 b at 20, 5, and 1 keV, respectively. These values we regard as larger than the (roughly) measured $(1+\alpha)\sigma_f$ and we think it unlikely that significantly larger penetration coefficients are reasonable. It will be observed that the larger coefficients become, at $E_n \simeq 10$ keV, the same as Beyster's at 20 keV. Thus if we multiply the cross sections to be reported by a factor two we obtain 10-keV cross sections with the larger T_i values. Since 10 keV is as good an energy for our

purposes as 20 keV and only cross section ratios will concern us here, the results may be viewed in either light.

C. Level Densities

In Eqs. (6), D_J is the parameter which varies the most as one considers different nuclei. Therefore we must consider its dependence on neutron-binding energy, spin, and odd-even effects with some care.

Level-density formulas for a Fermi gas have been considered by Bethe,²⁴ Lang and LeCouteur,²⁵ and Newton.⁹ We will be guided by the work of Newton, but will omit his considerations of closed-shell effects which are presumably unimportant for the nuclei under consideration. Following Newton, we define an effective excitation energy U' as equal to the actual excitation energy U minus a pairing correction

$$U' = U - \delta, \quad (7a)$$

where

$$\begin{aligned} \delta &= 0 \text{ for odd-odd compound nuclei,} \\ &= \frac{1}{2} \times 0.82 [4 - (A/100)] \text{ for even-odd and} \\ &\quad \text{odd-even compound nuclei,} \\ &= 0.82 [4 - (A/100)] \text{ for even-even compound nuclei.} \end{aligned} \quad (7b)$$

We have then taken

$$D_J = [D_0 / (2J+1)] e^{+(2J+1)^2/140} \quad (8)$$

and

$$D_0 = B(U')^2 e^{-a\sqrt{U'}}, \quad (9)$$

where we take B and a to be constants to be determined by fitting the data for heavy nuclei. We have also made a calculation of capture cross sections, omitting the exponential in Eq. (8). While this omission increases the difference between cross sections for even-even and those for all other nuclei, the results are qualitatively much the same as for the present prescription. We have also tried using $a \propto \sqrt{A}$, which does not fit the heavy-element data (in Table I) quite as well as $a = \text{const}$, but gives similar results.

To obtain the constants a and B we have assembled the level spacings, D_{obs} , for heavy nuclei which are observed with slow-neutron resonances.^{21,22} From these we estimate $D_0 = 2(2I+1)D_{\text{obs}} e^{-(2I+1)^2/140}$ for spin I target nuclei. The results are tabulated in Table I and $D_0(U')^{-2}$ is then plotted versus $\sqrt{U'}$ in Fig. 3. From this figure we deduce $a \simeq 7.5$, $B \simeq 3e^{15}$. The work of Lang and LeCouteur²⁵ and Newton⁹ on level-density formulas fitted to "all" nuclei would suggest somewhat larger values of a ($\simeq 9$) but we feel that our value is in better agreement with the data for heavy nuclei. Evidently even if one accepts the data of Table I and an expression of the form of Eq. (9) for D_0 , the pa-

²⁰ R. G. Schrandt, J. R. Beyster, M. Walt, and E. Salmi, Los Alamos Rept., LA-2099 (1957).

²¹ Brookhaven Report No. BNL-325, 1958 (unpublished).

²² J. D. Garrison, Ann. Phys. (N. Y.) **30**, 273 (1964).

²³ E. H. Auerbach and F. G. J. Perey, Brookhaven Report No. BNL-765, 1962 (unpublished).

²⁴ H. A. Bethe, Rev. Mod. Phys. **9**, 69 (1937).

²⁵ J. M. B. Lang and K. J. LeCouteur, Proc. Phys. Soc. (London) **A67**, 586 (1954).

TABLE I. Nuclear parameters. D_{obs} is observed level spacing and D_0 is the estimated level spacing for a spin-zero target nucleus. S_n is the neutron separation energy for the compound nucleus, and $U' = S_n - \delta$ with δ in Eq. (7).

| Target nucleus | I | D_{obs} (eV) ^a | D_0 (eV) | S_n (MeV) ^b | U' (MeV) |
|-------------------|---------------|------------------------------------|------------|--------------------------|------------|
| Th ²³² | 0 | 18.5 | 37 | 4.83 | 4.14 |
| U ²³³ | $\frac{5}{2}$ | 0.8 | 7.4 | 6.85 | 5.48 |
| U ²³⁴ | 0 | 14 | 28 | 5.31 | 4.63 |
| U ²³⁵ | $\frac{7}{2}$ | 0.6 | 6.1 | 6.49 | 5.14 |
| U ²³⁶ | 0 | 17 | 34 | 5.17 | 4.50 |
| U ²³⁸ | 0 | 19 | 38 | 4.85 | 4.19 |
| Np ²³⁷ | $\frac{5}{2}$ | 0.6 | 5.6 | 5.49 | 5.49 |
| Pu ²³⁹ | $\frac{3}{2}$ | 2.7 | 10.5 | 6.48 | 5.16 |
| Pu ²⁴⁰ | 0 | 14 | 28 | 5.24 | 4.63 |
| Pu ²⁴¹ | $\frac{5}{2}$ | 1.6 | 14.8 | 6.25 | 4.94 |
| Am ²⁴¹ | $\frac{5}{2}$ | 0.65 | 6.0 | 5.48 | 5.48 |
| Am ²⁴³ | $\frac{5}{2}$ | 1.2 | 11.1 | 5.35 | 5.35 |

^a See Ref. 22.
^b See Ref. 27.

parameter a is not very well determined, being uncertain to around ± 1 . Such an uncertainty is not very important for the qualitative conclusions of the present paper. In what follows we will use

$$D_J = \frac{3}{2J+1} e^{(2J+1)^2/140} (U')^2 \exp[-7.5[(\sqrt{U'})-2]], \quad (10)$$

where U' is in megaelectron volts and D_J in electron volts.

It has been recently suggested²⁶ that a simple ex-

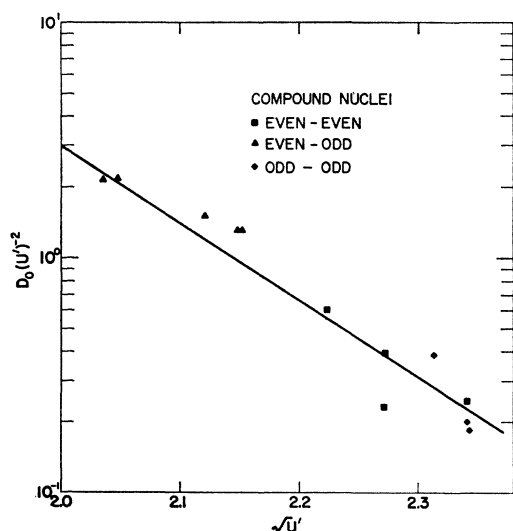


FIG. 3. Data of Table I are here plotted to determine the parameters a and B of Eq. (9). The straight line is the result for $a = 7.5$, $B = 3e^{+15}$.

²⁶ A. Gilbert, F. S. Chen, and A. G. W. Cameron, *Level Densities in Light Nuclei*, Goddard Space Flight Center Report, 1965 (unpublished).

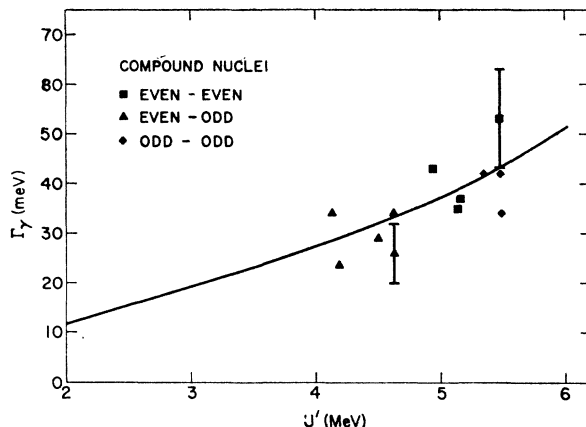


FIG. 4. Radiation widths versus effective excitation energy. The solid line is from Eq. (11) normalized to agree with the experimental points for heavy nuclei.

ponential level density might be more appropriate. We have therefore also fitted the data of Fig. 3 to the expression $D_0 = 48e^{-1.4(U'-4)}$ which happily agrees with our more complicated expression, Eq. (10), to within $\pm 20\%$ over the range of U' considered ($2 \leq U' \leq 5.7$). Since the prediction of level densities to within 20% is not possible at present we may regard the two level-density expressions as equivalent.

D. Radiation Width

Experimentally, the radiation width Γ_γ for heavy nuclei is nearly constant. In particular there is no marked dependence on spin and only a weak (if real) dependence on U' . The energy dependence of ξ_J is dominated by that of D_J and we have made one set of calculations assuming Γ_γ to be a constant, independent of U' . However in the results to be reported here we have taken a weak dependence on U' , as if levels decayed by electric dipole transition.¹⁹ This was calculated using

$$\Gamma_\gamma = \text{const} D_0(U') \int_0^{U'} \frac{E^3 dE}{D_0(U'-E)}, \quad (11)$$

with $D_0(U')$ given by Eq. (10) except that D_0 was taken constant for $U' \leq 0.5$. The results are shown in Fig. 4, together with experimental values²¹ which were used for normalization.

We have now determined all of the parameters for Eqs. (6) and can thus compute $\sigma_{n,\gamma}$ as the function of U' . For $E = 20$ keV, $I = 0$ and $I = \frac{5}{2}$, the results are shown in Fig. 5. For U²³⁸ and Th²³² ($U' = 4.2$,²⁷ $I = 0$) our calculated $\sigma_{n,\gamma}$ is 0.63 b, which is in reasonable agreement with experimental values²¹ which seem to center in the range from 0.5 to 0.6 b.

For neutron binding energies we have used the semi-

²⁷ M. Yamada and Z. Matumoto, J. Phys. Soc. Japan 16, 1496 (1961).

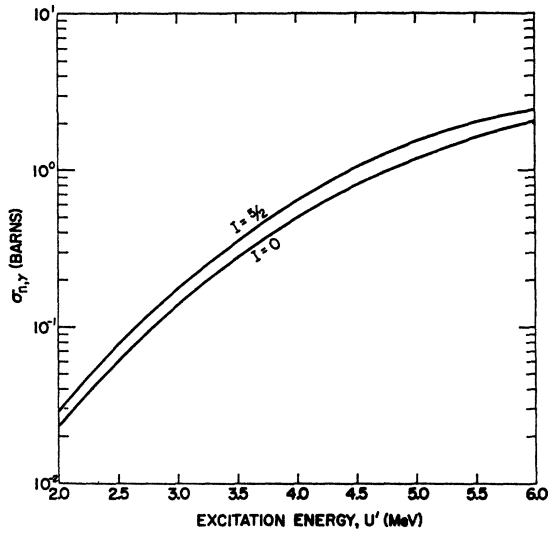


FIG. 5. Calculated radiative capture cross sections for neutrons of 20 keV versus effective excitation energy [see Eq. (7b)]. The $I=0$ curve is for even-even target nuclei while the $I=5/2$ curve was used for all other nuclei.

empirical mass tabulation of Seeger.¹⁰ [Seeger's recent revision (unpublished December 1964) of this tabulation yields neutron separation energies for isotopes of Pa, U, and Np in good agreement with his published¹⁰ values. The 1957 tables of Cameron²⁸ give binding energies which decrease at about the same rate with A , and hence quite similar results.] In view of the uncertainties in such semiempirical results, we neglect the neutron kinetic energy compared to the binding energy and thus take U' equal to the neutron separation energy minus δ .

TABLE II. Capture cross sections at 20 keV.

| A | Protoactinium | | Uranium | | Neptunium | |
|-----|---------------|-------------------------|---------------|-------------------------|---------------|-------------------------|
| | U' (MeV) | $\sigma_{n,\gamma}$ (b) | U' (MeV) | $\sigma_{n,\gamma}$ (b) | U' (MeV) | $\sigma_{n,\gamma}$ (b) |
| 238 | 4.91 | 1.44 | 3.92 | 0.46 | 5.74 | 2.25 |
| 239 | 4.05 | 0.68 | 4.52 | 1.06 | 4.85 | 1.38 |
| 240 | 4.66 | 1.20 | 3.65 | 0.34 | 5.45 | 1.98 |
| 241 | 3.79 | 0.51 | 4.26 | 0.84 | 4.55 | 1.10 |
| 242 | 4.42 | 0.97 | 3.38 | 0.24 | 5.16 | 1.70 |
| 243 | 3.55 | 0.38 | 4.01 | 0.65 | 4.27 | 0.84 |
| 244 | 4.20 | 0.79 | 3.14 | 0.17 | 4.89 | 1.41 |
| 245 | 3.33 | 0.28 | 3.79 | 0.51 | 4.00 | 0.64 |
| 246 | 3.99 | 0.64 | 2.91 | 0.12 | 4.64 | 1.18 |
| 247 | 3.12 | 0.21 | 3.58 | 0.40 | 3.75 | 0.48 |
| 248 | 3.81 | 0.52 | 2.70 | 0.086 | 4.42 | 0.97 |
| 249 | 2.94 | 0.16 | 3.38 | 0.30 | 3.52 | 0.37 |
| 250 | 3.64 | 0.42 | 2.51 | 0.062 | 4.20 | 0.79 |
| 251 | 2.77 | 0.12 | 3.21 | 0.24 | 3.31 | 0.28 |
| 252 | 3.48 | 0.35 | 2.33 | 0.044 | 4.00 | 0.64 |
| 253 | 2.62 | 0.096 | 3.05 | 0.19 | 3.11 | 0.21 |
| 254 | 3.35 | 0.29 | 2.17 | 0.032 | 3.82 | 0.52 |
| 255 | 2.48 | 0.075 | 2.91 | 0.15 | 2.93 | 0.16 |
| 256 | 3.22 | 0.24 | 2.03 | 0.024 | 3.66 | 0.44 |
| 257 | 2.35 | 0.058 | 2.78 | 0.13 | 2.77 | 0.12 |

²⁸ A. G. W. Cameron, Atomic Energy of Canada, Chalk River Report CRP-690, 1957 (unpublished).

In Table II are presented the values of U' and $\sigma_{n,\gamma}$ (as found from Fig. 5), for nuclei having $Z=91, 92, 93$, and $238 \leq A \leq 257$.

IV. COMPARISON WITH EXPERIMENT

In Sec. II, we estimated that the fast neutron flux would be responsible for production of about 10^{-3} Pa/U and $\lesssim 10^{-3}$ Np/U, where these are ratios of nuclei which survive the fast flux. We have also calculated capture cross sections for the nuclei of interest at a neutron energy of 20 keV, where this neutron energy is taken to be representative of the neutron energies after thermalization. Neither the actual spread of neutron energies, nor possible departures of the average energy from 20 keV will have important effects on our conclusions. If $\varphi(t)$ is the time integrated flux of thermal neutrons [$\varphi(t) = \int' n v d t'$], N_i is the number of $238+i$ nuclei (for fixed Z), and σ_i is the (n,γ) cross section of these nuclei, then

$$dN_i/d\varphi = \sigma_{i-1}N_{i-1} - \sigma_i N_i. \quad (12)$$

We have one such equation for each nuclide under consideration.

W. Anderson of this Laboratory has prepared a code to numerically solve Eq. (12) for $0 \leq i \leq 40$, starting from prescribed initial conditions. We have obtained solutions for the mass chains, starting from U^{238} , Pa^{238} , and Np^{238} (ignoring fission).

In fitting the experimental data^{2,3} given in Table III from Barbel and Par, we have treated the thermal flux, $\varphi(\infty) = \varphi$, as a variable and the amounts of U, Pa, and Np which are exposed to the thermal flux as variable within limits. However, using the cross sections of Table II, we are able to obtain good agreement with experiment only for a narrow range of fluxes and target abundances. In particular, a fit to the low-mass end of the mass curve $243 \leq A \leq 248$ can only be ob-

TABLE III. Abundances of mass-A nuclei relative to initial uranium-238.

| A | $N(A)/N_0(U^{238})$ | | | |
|-----|---------------------------|-------------------------|---------------------------|-------------------------|
| | Par | | Barbel | |
| | Experimental ^a | Calculated ^b | Experimental ^c | Calculated ^d |
| 244 | | | 2.3×10^{-3} | 3.2×10^{-3} |
| 245 | 10^{-3} | 1.8×10^{-3} | 3.7×10^{-4} | 5.3×10^{-4} |
| 246 | 8.5×10^{-4} | 1.1×10^{-3} | 2.6×10^{-4} | 3.2×10^{-4} |
| 247 | 1.1×10^{-4} | 1.3×10^{-4} | 3.1×10^{-5} | 3.5×10^{-5} |
| 248 | 5.1×10^{-5} | 4.6×10^{-5} | 1.2×10^{-5} | 1.2×10^{-5} |
| 249 | 9×10^{-6} | 1.2×10^{-5} | 2.2×10^{-6} | 2.1×10^{-6} |
| 250 | 4.1×10^{-6} | 2.9×10^{-6} | 5.9×10^{-7} | 5.1×10^{-7} |
| 251 | $\leq 1.3 \times 10^{-6}$ | 1.7×10^{-6} | ... | 2.5×10^{-7} |
| 252 | 2.2×10^{-7} | 2.8×10^{-7} | 5.3×10^{-8} | 4.2×10^{-8} |
| 253 | 1.1×10^{-7} | 1.2×10^{-7} | 2.2×10^{-8} | 1.8×10^{-8} |
| 254 | 1.2×10^{-8} | 1.3×10^{-8} | 1.8×10^{-9} | 1.9×10^{-9} |
| 255 | 4.3×10^{-9} | 3.8×10^{-9} | 9.1×10^{-10} | 5.7×10^{-10} |
| 256 | 2.6×10^{-10} | 2.8×10^{-10} | ... | 4.1×10^{-11} |
| 257 | 5.6×10^{-11} | 5.9×10^{-11} | 1.3×10^{-11} | 8.8×10^{-12} |

^a Data from Ref. 2 normalized to $N(245)/N_0(U^{238}) = 10^{-3}$ from Ref. 3.

^b Calculated with same assumptions as for Fig. 6.

^c Data from Ref. 3.

^d Calculated with same assumptions as for Fig. 7.

tained using the uranium chain, target abundances ~ 0.1 initial uranium, and $\varphi \approx 7 \times 10^{24}/\text{cm}^2$. The high mass end $A > 249$ can be fit with the same flux using the Np chain with $\text{Np}/\text{U} \approx 10^{-3}$ for Par and 5×10^{-4} for Barbel. The Pa chain cannot contribute at all unless one is willing to admit substantially higher fluxes in the Pa ($\varphi \sim 10$) and an embarrassing amount of Pa ($\text{Pa}/\text{U} \sim 10^{-2}$) in which case a fair fit can be obtained to the high-mass data.

The comparison between these fits and experiment is shown in Fig. 6 for Par and in Fig. 7 for Barbel. It is to be noted^{2,3} that the mass 243 and 244 experimental points are perhaps somewhat too high because an appreciable fraction of these isotopes may have been produced elsewhere in the device. From Figs. 6 and 7 we observe good general agreement between the experimental and calculated abundances.

From this agreement we conclude that the Par and Barbel (and Mike) data can be understood on the basis of conventional mass formulas and neutron capture theory. The higher mass isotopes ($A \gtrsim 249$) are then interpreted as resulting from capture in odd- Z mass chains, most likely Np.

It is then natural to ask whether this general agreement depends sensitively on the particular cross sections which we have calculated and presented in Table II. During the course of this study we have considered several variants on the basic method for calculating

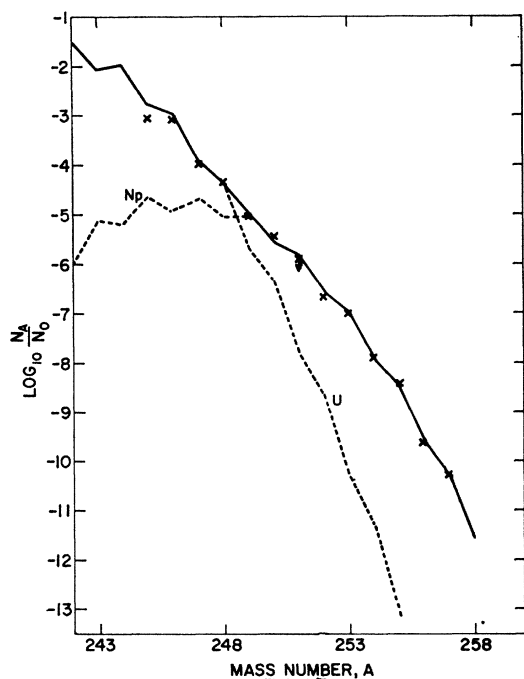


FIG. 6. Mass abundance versus mass number for the Par device. For the calculation it was assumed that the time-integrated flux of 20-keV neutrons was $7 \times 10^{24}/\text{cm}^2$ and the amounts of uranium and neptunium exposed were 10^{-1} and 10^{-4} of the initial uranium, respectively. The dashed lines show contributions of the uranium and neptunium fractions separately.

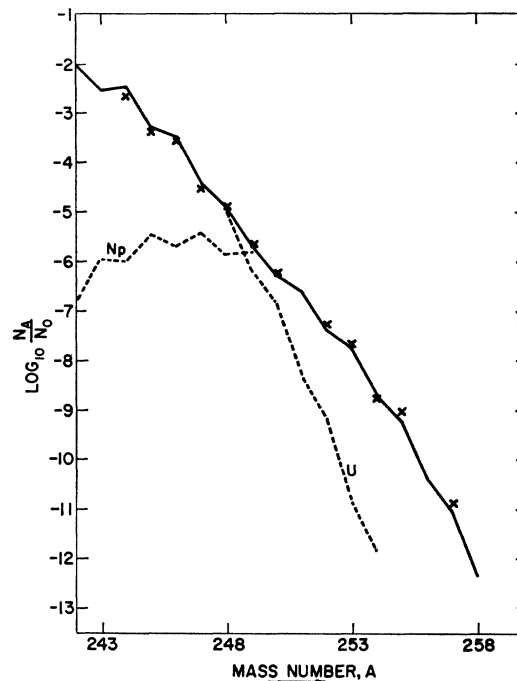


FIG. 7. Mass abundance versus mass number for the Barbel device. For the calculation it was assumed that the time-integrated neutron flux was $7 \times 10^{24}/\text{cm}^2$ and the amounts of uranium and neptunium exposed were 3×10^{-2} and 1.5×10^{-5} of the initial uranium, respectively.

$\sigma(n, \gamma)$. In particular, as mentioned previously, we considered (1) several variations of our level density formula, Eq. (10), (2) constant Γ_γ versus variable Γ_γ , and in addition we have considered (3) several neutron energies $1 \text{ keV} \leq E_n \leq 20 \text{ keV}$ and (4) a recent²⁹ and unconventional (exponential) binding energy tabulation of Cameron. In none of the cases considered was it possible to obtain a reasonable fit to the data from Par and Barbel by using only capture in uranium. Always the calculated abundances of high- A isotopes were too low. In each case a fair fit to the data could be obtained by allowing capture in odd Z isotopes. To fit the Par data, ratios $\text{Np}/\text{U} \sim 10^{-3}$ with the flux in the Np equal to or slightly less than that in the U were required; or else $\text{Pa}/\text{U} \sim 10^{-2}$ with the fluxes in the Pa somewhat (20%–50%) higher than in the U. For Barbel the required odd- Z abundances are about a factor two lower.

We thus conclude that the general picture of the capture process in Par and Barbel is insensitive to many of the details of the $\sigma(n, \gamma)$ calculation. Of course, from comparing in detail the calculated and experimental results one should be able to draw some conclusions regarding acceptable ranges of $\sigma(n, \gamma)$. Alternatively one could try to deduce $\sigma(n, \gamma)$ values directly from the abundance curves, as has been attempted by

²⁹ A. G. W. Cameron and R. M. Elkin, Goddard Institute for Space Studies report, 1964 (unpublished).

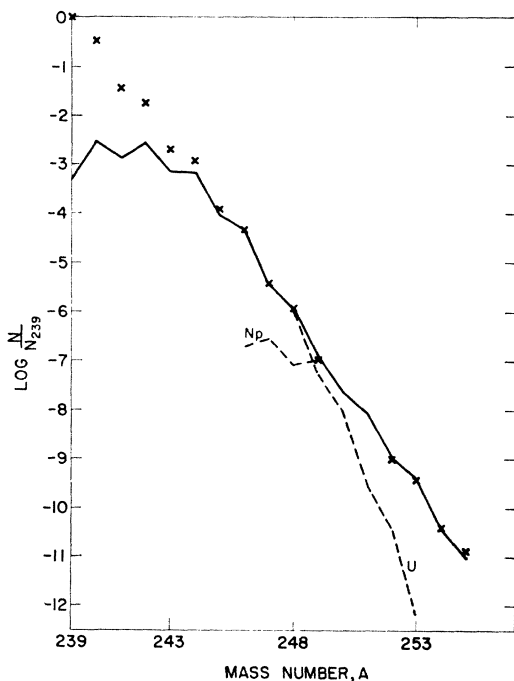


FIG. 8. Mass abundance versus mass number for Mike. Data from Ref. 1, except that the mass-255 point of Ref. 1 has been decreased by a factor 4 to take into account more recent information on the decay chain [H. Diamond (unpublished)]. In the calculation, $\phi = 6 \times 10^{24}$ and the uranium exposed to this flux is 10^{-2} times the remaining U^{239} while the neptunium was 1.5×10^{-6} times the remaining U^{239} .

Ingley,³⁰ Such detailed comparisons, however, are beyond the scope of the present paper.

³⁰ J. S. Ingley (to be published), and Ref. 2.

It is also interesting to see to what extent the Mike data¹ can be understood in the present context. It is first of all evident that some of the low- A data points (in particular the data for masses 239, 240, 241, 242, and possibly also 243 and 244) must be disregarded as resulting from capture in low flux regions. It is then found that the data for $245 \leq A \leq 249$ can be fit by a uranium chain with $\phi = 6 \times 10^{24}$ while the points $252 \leq A \leq 254$ are obtained from an Np chain with $Np/U = 1.5 \times 10^{-4}$. The results are shown in Fig. 8.

It is to be noted that in our analysis, spontaneous fission has been ignored. In a recent interpretation of Par data, based on capture in uranium isotopes only, Dorn has suggested² that the reversal of odd-even effects for $A \geq 250$ may indicate a competition between spontaneous fission and β decay of the even- A chains. If we accept the reversal of odd-even effects as a direct consequence of capture in odd- Z nuclei there remains no evidence for spontaneous fission and we may conclude that the spontaneous fission lifetimes are longer than β decay lifetimes.

ACKNOWLEDGMENTS

The author wishes to thank Dr. William Gibbs for calculations of the relative (d,n) and (d,p) cross sections and William Anderson of this Laboratory for programming the solution of Eqs. (12) for solution by the IBM-7094 computer. He is also indebted to A. G. W. Cameron for communicating results on semi-empirical separation energies and level densities, prior to publication. It is a pleasure to acknowledge helpful conversations with J. Carson Mark, George Cowan, and Albert Petschek.